Journal of Chemical&Engineering Data

pubs.acs.org/jced Article

Investigating Aqueous Two-Phase Systems Constituted by Benzyltributylammonium Chloride-Based Deep Eutectic Solvents for Efficient Extraction of Textile Dyes

Published as part of Journal of Chemical & Engineering Data special issue "Aqueous Two-Phase Systems for Separation Processes: From Fundamental Data to Applications".

Nensi A. Patel, Emmanuel A. Oke, and Sushma P. Ijardar*

Cite This: *J. Chem. Eng. Data* 2025, 70, 3364−3377 Read Online

ACCESS | Metrics & More | Article Recommendations | Supporting Information

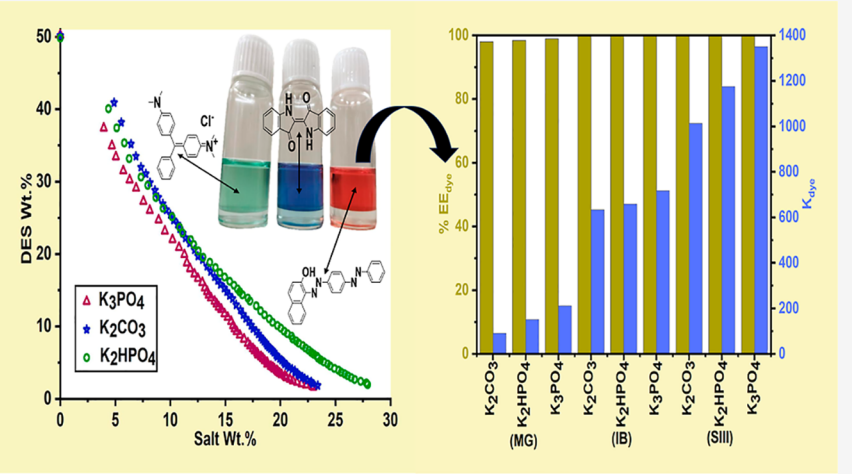

ABSTRACT: Aqueous two-phase systems (ATPS) have been considered as an eco-friendly separation system for the extraction of value-added compounds from an aqueous matrix. Deep eutectic solvents (DESs) have been used as the latest phase - forming component in ATPS. The novel DES-based ATPS composed of DESs and with K_3PO_4, K_2HPO_4, and K_2CO_3 were investigated at 298.15 K and atmospheric pressure. DESs were synthesized using benzyltributylammonium chloride (BTBAC) with methanol, ethanol, propanol, and polyethylene glycol (PEG) of average molar mass: 200, 400, and 600 in a 1:3 molar ratio. The ability of the studied salt to induce phase separation follows the order: $K_3PO_4 > K_2HPO_4 \approx K_2CO_3$. The investigated ATPS were evaluated as an extraction platform for malachite green (MG), indigo blue (IB), and Sudan III (SIII) from aqueous solutions. The highest partition coefficients (K_{dyes}) 211.01, 716.91, and 1350.35 were observed for MG, IB, and SIII, respectively, using BTBAC:PEG 600 and K_3PO_4 ATPS. The highest extraction efficiencies (EE_{dye} %) around 100% were reported for all studied dyes by the same ATPS. The extraction capacity of studied ATPS depends upon log K_{ow} values and functional groups present in the dye structure. The obtained results highlight the potential use of DES-ATPS in the purification of dye containing wastewater.

1. INTRODUCTION

Global population growth is driving the demand for several basic materials on a daily basis. The tenets of green chemistry have suggested an appropriate disposal of the contaminants.[1] Environmental contamination has increased drastically due to urbanization and rapid socioeconomic advancement.[2,3] The effluents released by industries contain significant amounts of harmful chemical contaminants into the environment. The textile industries produce large quantity of materials used to impart color known as dyes. More than 70 million tons of dyes are produced every year worldwide. The textile industries utilize around 10,000 tons of annually produced dyes. It is reported that around 50% of the dyes used by the textile industry belong to azo dyes. However, these dyes could not react completely with the fiber and 28,000 tons of dyes containing wastewater is being

Received: May 29, 2025
Revised: July 12, 2025
Accepted: July 29, 2025
Published: August 5, 2025

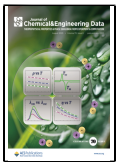

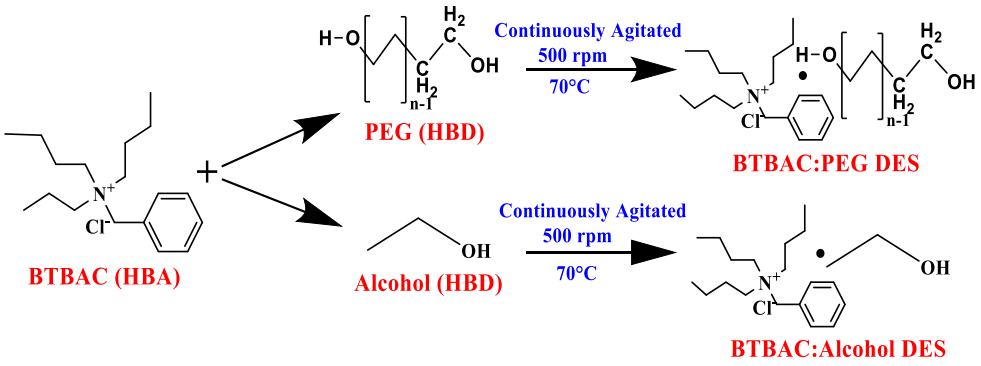

Figure 1. Synthesis of the DESs used in this study.

discharged on surface or groundwater.[4,5] The use of dye containing water leads to several human and animal diseases and environmental deterioration.[5,6] Apart from the above-mentioned factors, aquatic organisms have been adversely effected by the presence of dye.[7,8] Therefore, the removal of dyes from water and wastewater becomes essential.

Several separation methods have been employed to extract dyes from wastewater. The methods are generally categorized as chemical, physical, or biological techniques like liquid extraction, oxidation, photodegradation, adsorption, ozonation, membrane processes, and chemical/biological degradation.[9,10] Each technique has its own benefits and drawbacks. For instance, photodegradation and chemical processes utilize toxic chemicals and produce more toxic chemicals than the original when they degrade during the process.[11] The adsorption process requires a longer adsorption time. As a result, liquid−liquid extraction has been preferred as the recommended strategy for the extraction of dyes among the techniques mentioned. Liquid−liquid extraction is a popular, effective, and straightforward method that requires less time than all other available techniques.[12] Aqueous two-phase systems (ATPS) or aqueous biphasic systems (ABSs) have been considered an efficient method for the separation of dyes and other compounds from wastewater.[12,13]

ATPS have been recognized as greener systems for the possible extraction and separation of compounds. They are considered as biocompatible system as two immiscible phases are mainly composed of water.[14,15] The three-component systems can exist in equilibrium in two phases under specific composition, temperature, and pressure conditions. ATPS are regarded as nonflammable and scalable systems due to the concentration of their components.[14,16] Two distinct water-soluble components, inorganic salt, polymers, amino acids, surfactants, ionic liquids (ILs), and sugars were used in the fabrication of ATPS and have been used for the extraction and purification of a broad array of compounds like enzymes, proteins, amino acids, phytochemicals, pesticides, metals, and dyes.[2,13,17]

Deep eutectic solvents (DESs) have been considered as one of the components of ATPS to develop environmentally friendly separation processes.[18,19] DESs are composed of two or three low-cost components that can combine to form a eutectic mixture through hydrogen bond interactions. DESs are typically prepared by combining a hydrogen bond donor (HBD) and a hydrogen bond acceptor (HBA) in a specific molar ratio. The growing popularity of DESs is attributed to their unique qualities such as being less hazardous, biodegradable, easier to prepare on large scale, less expensive, and "green" as compared to ILs and volatile organic solvents.[20−22] The construction of novel DESs-based ATPS with polymers, carbohydrates, and organic and inorganic salts has been the subject of research during past few years.[17−19,23]

The possibility of ChCl−urea DES as a phase-forming component for ATPS was first investigated in 2014 by Zeng et al. and successfully demonstrated for the extracted bovine serum albumin.[24] Following this work, ChCl:glucose + K_2HPO_4 was studied by Farias and his associates for protein extraction.[25] Yin and co-workers used betaine−xylitol DES-based ATPS with 1-propanol/2-propanol/*tert*-butanol to extract five bioactive compounds (gallic acid, syringic acid, quercetin, kaempferol, and isorhamnetin).[26] DES-based ATPS have been successfully employed in the extraction and purification of various biomolecules.[13,17] Recently, Li and his research group[27] investigated a new green ABS containing ethyl lactate (EL) and hydrophilic sugar-based DES for the extraction of biomolecules such as rutin, gallic acid, vanillin, and eugenol. The hydrophilicity gap between sugar-based DES and EL increases with increases in the number of hydroxyl groups in sugar, leading to improved phase-forming capacity of DESs. Eugenol, vanillin, and vanillic acid were partitioned into the hydrophobic EL-rich phase, whereas rutin and gallic acid moved into the hydrophilic DES-rich phase.

The application of DES-based ATPS for the extraction of dyes has not been explored much in the literature. Xu et al.[28] introduced benzyl-based quaternary ammonium salts−glycerine DES-based ABSs for the extraction of Sudan III, sunset yellow FCF, amaranth, and tartrazine from aqueous media. ATPS observed the selective separation from the mixed sample. 98.47% of Sudan III and 99.47% of tartrazine were partitioned into the PPG-rich phase and DES-rich phase, respectively. Furthermore, the study effectively extracted pigments from real beverage samples with recovery rates 93.43% and 102.15%. Sudan III and pigment blue were completely extracted using choline chloride:carboxylic acids DESs + PPG 400.[29] Natural DES-based micellar ATPS were studied for the extraction of methylene blue, Sudan III, and sunset yellow FCF.[30] More than 95.00% extraction efficiencies were observed for Sudan III, tartrazine, and methylene blue by DES-based ATPS.[31] ATPS composed of tetrabutylammonium bromide: PPG 400 DES, and citrate salts were studied for extraction of congo red, methylene blue, and methyl orange from aqueous solution with more than 98.00% efficiency.[32] Alizarin red S, orange II, congo red, methyl orange, eriochrome black T, and eosin Y were extracted by benzyltrialkylammonium chloride and alcohol/glycol-based DES with K_3PO_4.[33−35] Asla et al.[36] and Martínez-Rico et al.[37] explored the potential of tetrabutylammonium chloride−

https://doi.org/10.1021/acs.jced.5c00346
J. Chem. Eng. Data 2025, 70, 3364−3377

decanoic acid-based DESs for the separation of dyes from aqueous medium. Recently, hydrophobic deep eutectic solvents have been used in the identification and extraction of organic pollutants, petrochemical products, phenolic pollutants, and metals from aqueous media.[38−42]

Considering the above potential of ATPS as an efficient separation system and continuation of our research work on ATPS, this work aims to develop new ATPS using benzyltributylammonium chloride (BTBAC)-based DESs and potassium salts at 298.15 K for the extraction of dyes. The choice of BTBAC as HBA was based on its aromatic nature to facilitate the possible interaction with dyes and to improve the hydrophobicity of DES for phase separation.[34,35] Propanol (PROH), ethanol (ETOH), and methanol (MEOH), as well as polyethylene glycol (PEG) 200, 400, and 600 were chosen as HBDs to further increase the hydrophobicity of DESs. The salts (K_3PO_4, K_2HPO_4, and K_2CO_3) were used for their higher capacity to induce phase separation compared to their organic counterparts.[30,31] The constructed DES-based ATPS were investigated for their ability to extract malachite green (MG), indigo blue (IB), and Sudan III (SIII) from an aqueous matrix at atmospheric pressure and 298.15 K. In the literature, no data have been reported for BTBAC:alcohol and BTBAC:PEG-based ATPS and application in the extraction of these dyes. This study will benefit the field of environmental science to extract dyes and other contaminants from water/wastewater.

2. EXPERIMENTAL AND/OR COMPUTATIONAL METHODS

2.1. Chemicals. BTBAC (purity = 98 wt %) was obtained from Spectrochem Pvt. Ltd. India. K_3PO_4 (purity ≥98 wt %), K_2HPO_4 (purity ≥98 wt %), K_2CO_3 (purity ≥98 wt %), MG (purity = 98 wt %), IB dye (purity >95 wt %), Sudan III dye (purity >99 wt %), PEG 200, PEG 400, and PEG 600 (purity = 99.50 wt %) were purchased from Merck, India. Methanol (purity ≥99.80 wt %), ethanol (purity ≥99.50 wt %), and propanol (purity ≥99.50 wt %) were acquired from Thermo Fisher Scientific. All chemicals were used as provided by the supplier without any further purification. Deionized water was used for solution preparation. Further information about each chemical used in this investigation is included in Table S1. The structures of the studied dyes are displayed in Figure S1.

2.2. Preparation and Characterization of DESs. The six DESs utilized in this investigation were synthesized as shown in Figure 1 using benzyltributylammonium chloride (BTBAC) as HBA and methanol (MEOH), ethanol (ETOH), propanol (PROH), and polyethylene glycol (PEG) 200, 400, and 600 as HBDs. The HBA and HBD of DES were precisely weighed at a 1:3 molar ratio and agitated (500 rpm) at 70 °C and atmospheric pressure until a clear, uniform liquid was obtained. The synthesized DESs were kept in a desiccator to absorb any moisture from the surrounding air. The water content of the prepared DES was determined using Karl Fischer, and the water content of around 1% was noticed for all studied DESs. The FT-IR spectra of the prepared DESs were recorded with a Shimadzu Fourier transform infrared spectrophotometer -8400S in the 400−4000 cm^{-1} region.

2.3. Characterization of DESs by FT-IR Spectroscopy. The FT-IR analytical method was used to identify the functional groups present in the synthesized DESs. The IR spectra of DESs clearly indicate the presence of hydrogen bonding with reference to stretching band vibrations of the −OH group (Figure 2A,B). The broad stretching bands in the 3700−3100 cm^{-1} region are

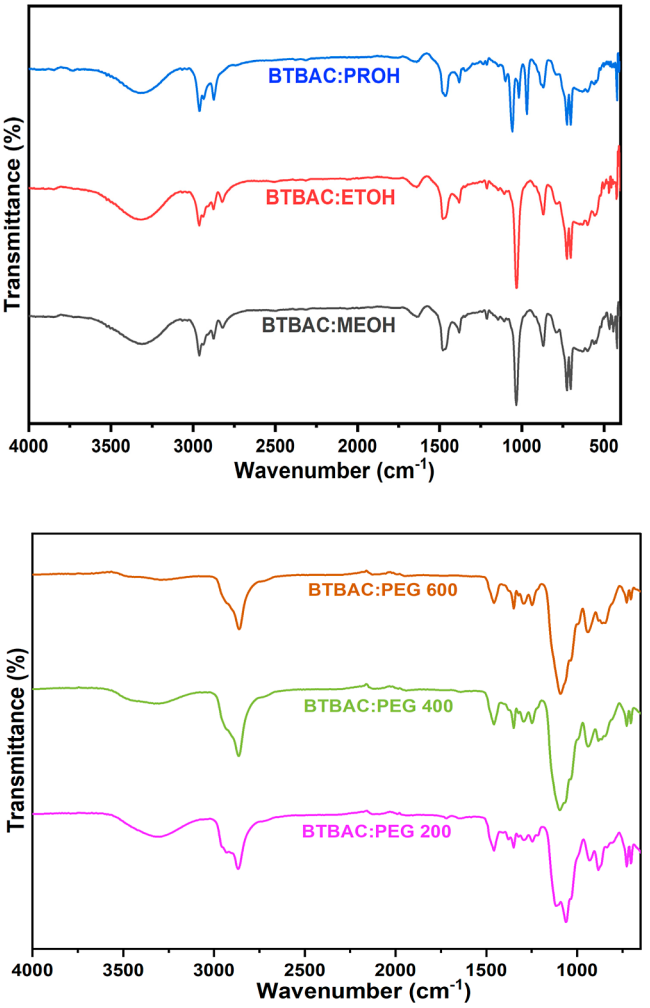

Figure 2. FT-IR spectra of the investigated (A) alcohol-based DESs, (B) PEG-based DESs.

associated with the presence of an −OH group.[33] The degree of hydrogen bonding between the halide anion of BTBAC (HBA) and alcohol/PEG (HBD) has a considerable impact on these bands and causes them to shift from upper or lower wavenumbers.[43] In other words, stretching of the −OH at 3340−3320 cm^{-1}, aromatic at 3100−3050 cm^{-1}, aliphatic at 2950−2900 cm^{-1}, C═C ring stretching at 1650−1640 cm^{-1}, and C−C ring stretching at 1480−1470 cm^{-1}, respectively, can be observed in spectra of DESs. Additionally, C−OH bending, C−O and C−O−C stretching, −OH wagging, and aromatic −CH wagging can be observed at 1390 cm^{-1}, 1060−1030 cm^{-1}, 910−890 cm^{-1}, and 750−700 cm^{-1}, respectively.

2.4. Fabrication of Phase Diagrams. The phase diagram in this investigation was obtained using the turbidimetric titration method. The binodal curves for studied DES-based ATPS (BTBAC:alcohols/PEGs + K_3PO_4/K_2HPO_4/K_2CO_3) were determined at 298.15 K with atmospheric pressure using the cloud point titration method.[33] In the case of alcohol-based DES, 60 wt % DES + 40 wt % salt solution and 50 wt % DES + 50 wt % salt solutions were used for polymer based DES to get two-phase formation. First, a known amount of DES solution was taken in clear vial, and salt solution was carefully added to get turbidity, followed by dropwise addition of distilled water to get clear solution. Again, an aqueous salt solution was added to get turbidity. The amount of DES and salt required to create a two-

https://doi.org/10.1021/acs.jced.5c00346
J. Chem. Eng. Data 2025, 70, 3364−3377

Table 1. Weight Fraction Compositions for Salt (X) and DES (Y) in the Mixture (M), Bottom Phase (B), and Top Phase (T), and Corresponding TLLs for Studied DES-Based ATPS at 298.15 K and Atmospheric Pressure[a]

DES	salt	X_M	Y_M	X_B	Y_B	X_T	Y_T	TLL
BTBAC:MEOH	K_3PO_4	30.24	7.51	47.51	2.52	7.52	18.5	43.08
	K_2HPO_4	30.58	7.58	45.54	2.71	4.74	24.5	46.26
	K_2CO_3	30.22	8.22	47.93	3.24	8.05	28.5	47.35
BTBAC:ETOH	K_3PO_4	30.45	6.51	41.54	3.51	7.75	18.21	36.73
	K_2HPO_4	30.54	9.23	42.91	5.24	13.02	17.92	32.56
	K_2CO_3	30.13	7.54	44.56	3.35	13.10	19.95	35.52
BTBAC:PROH	K_3PO_4	30.23	5.15	45.12	1.95	9.25	15.16	38.19
	K_2HPO_4	30.21	6.54	45.53	2.95	9.84	16.95	38.35
	K_2CO_3	30.15	5.51	50.51	1.85	5.25	17.70	47.95
BTBAC:PEG 200	K_3PO_4	30.25	9.25	40.8	4.75	3.19	26.95	43.67
	K_2HPO_4	30.21	11.25	41.05	8.05	4.05	28.15	42.11
	K_2CO_3	30.25	9.72	39.93	5.85	4.57	28.50	41.99
BTBAC:PEG 400	K_3PO_4	30.25	6.95	40.05	3.05	4.15	19.45	39.47
	K_2HPO_4	30.15	8.54	40.95	4.52	3.45	21.55	41.19
	K_2CO_3	30.05	7.95	40.05	4.35	4.80	24.25	40.48
BTBAC:PEG 600	K_3PO_4	30.05	5.65	40.05	2.50	3.5	17.75	39.60
	K_2HPO_4	29.95	6.65	40.15	3.75	6.45	19.35	37.14
	K_2CO_3	30.15	6.95	40.15	3.85	3.11	19.85	40.31

[a]The standard uncertainties (u) for temperature, pressure, and TLL are $u(T) = \pm 0.05$ K, $u(p) = \pm 0.5$ kPa, and $u(\text{TLL}) = \pm 0.007$, respectively.

phase system was obtained by subtracting the weight of empty glass vials from the respective weight of vials at each step. The above process was carried out multiple times until the necessary amount of data was collected for the binodal curve. The wt % of DES and salt was determined using the Mettler Toledo JE1103CE (Switzerland) analytical balance with an uncertainty of $\pm 10^{-4}$ g.

To validate the correctness of the cloud point method used to study the binodal curve in the present investigation, three ATPS composed of PEG 6000 + Na_2HPO_4, PEG 600 + K_3PO_4, and PEG 400 + K_2CO_3 have been studied at 298.15 K. The choice of these systems was based on the availability of the data in the literature. The binodal curve data for all three systems are listed in Table S2. The comparison between experimental and literature data for the binodal curve for all three systems is graphically depicted in Figure S2. The shape of the binodal curve is similar for all studied systems; however, a slight deviation was observed due to differences in composition of the components and the accuracy of the balance used in the cloud point measurement. The standard deviation between experimental and literature values for Figure S2 (a, b, and c) are 0.36, 0.87, and 1.70 (for common x values) and 3.29, 1.97, and 6.71 (for common y values).

The empirical eq 1 by Merchuk et al. was used to fit experimental results for binodal curve data.[44]

$$Y = A \exp[(B \times X^{0.5}) - (C \times X^3)] \quad (1)$$

The fitting parameters A, B, and C were derived from the least-squares regression of the experimental data. Y and X represent weight fraction percentages of DES and salt, respectively. The numerical values of the constants A, B, and C are listed in Table S3.

2.5. Determination of TieLines (TLs). The points for the TLs were obtained from the biphasic region of the phase diagram. The respective quantities of system components were obtained by weighing them into centrifuge bottle and stirring at 2500 rpm for around 30 min. The centrifuge tubes were allowed to acclimate at 298.15 K in a water bath. The top and bottom phases were separated carefully, and the appropriate weights were recorded. The following four equations 2−5 were utilized to get an accurate estimate of the TLs.

$$Y_T = A \exp[(B \times X_T^{0.5} - C \times X_T^3)] \quad (2)$$

$$Y_B = A \exp[(B \times X_B^{0.5} - C \times X_B^3)] \quad (3)$$

$$Y_T = \frac{Y_M}{\alpha} - \frac{1-\alpha}{\alpha} \times Y_B \quad (4)$$

$$X_T = \frac{X_M}{\alpha} - \frac{1-\alpha}{\alpha} \times X_B \quad (5)$$

The tie-line lengths (TLLs) were calculated by eq 6, and the values obtained for TL compositions are presented in Table 1. A TLL is a numerical representation of the variation in the top and bottom phase concentrations when two phases have been equilibrated. This is useful in selecting the right composition of salt and DES to extract the desired compounds from an aqueous matrix.

$$\text{TLL} = \sqrt{(X_T - X_B)^2 + (Y_T - Y_B)^2} \quad (6)$$

The X_T, X_B, and X_M represent the weight fraction percentage for salt in the top phase, bottom phase, and primary mixture. The weight fraction percentage for DES in the top phase, bottom phases, and primary mixture is represented by Y_T, Y_B, and Y_M. α denotes the weight ratio of the top phase to total weight of the mixture, and the fitting constants of eq 1 are represented by letters A, B, and C.

2.6. Extraction of Dyes. To examine the extraction capacity of the fabricated DES-based ATPS, three types of dyes (MG, IB, and SIII) with varying hydrophobic properties were chosen as the compounds of interest. A 15 mL transparent glass bottle was filled with a known amount of DES, salt, and dye solution of 400 mg/L concentration. The mixture was then agitated vigorously for approximately 5 min at 400 rpm in order to improve the equilibrium and efficiency of the extraction platform. After that, the mixture was left in a water bath at 298.15 K for 24 h in order to equilibrate. The top phase (DES-rich containing dye) and the bottom (salt-rich) phases were separated carefully by using a

https://doi.org/10.1021/acs.jced.5c00346
J. Chem. Eng. Data 2025, 70, 3364−3377

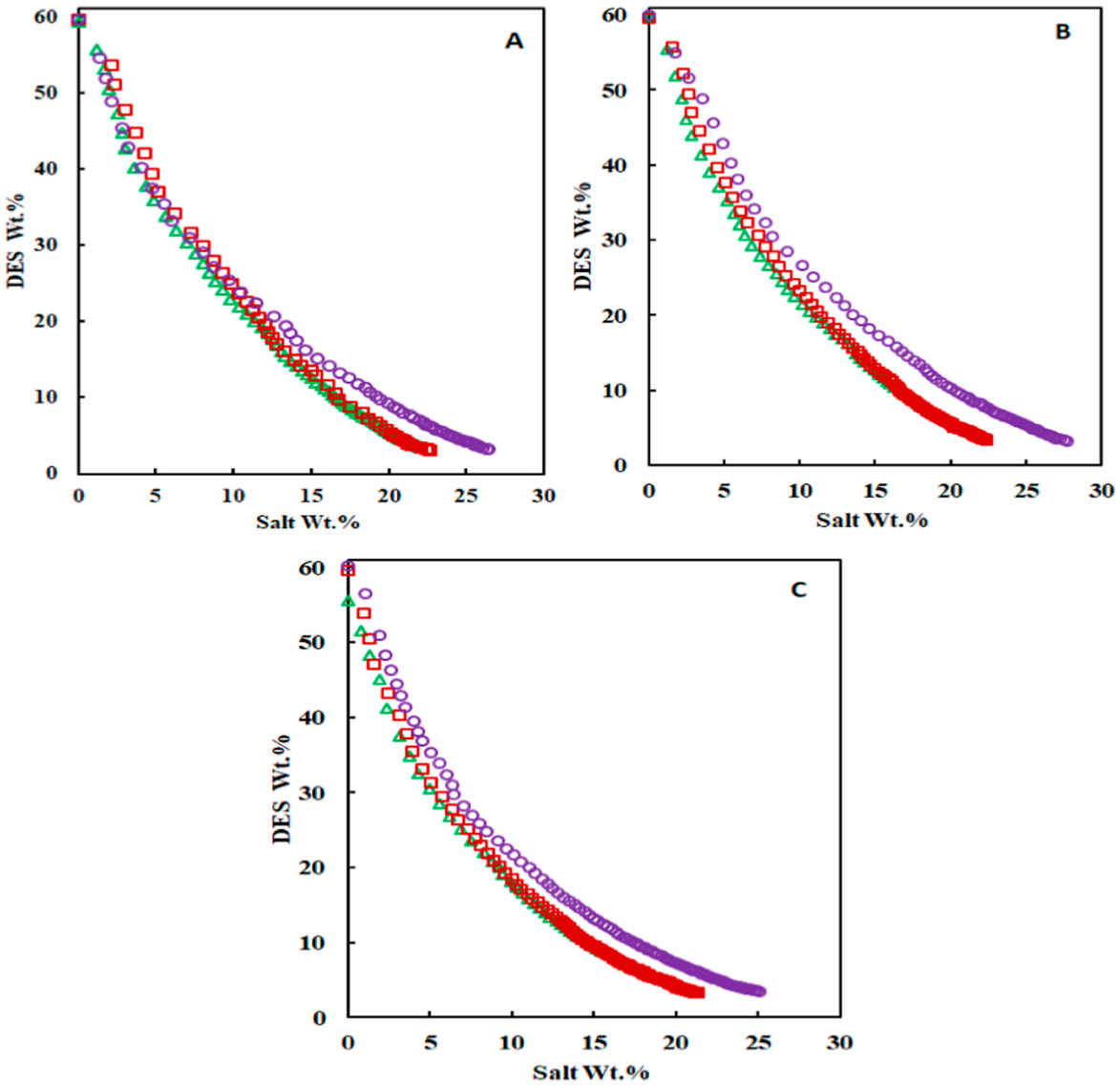

Figure 3. Effect of inorganic salts **green Δ: K_3PO_4 violet O: K_2HPO_4, red □: K_2CO_3** on the phase behavior of various DES:alcohol-based ATPS at 298.15 K and atmospheric pressure. (A) BTBAC:MEOH, (B) BTBAC:ETOH, (C) BTBAC:PROH. The plots are drawn using data presented in Tables S4−S6.

syringe. The absorbance measurements of diluted solutions of MG, IB, and SIII dyes were observed at 620, 335, and 338 nm, respectively, using a UV−visible spectrophotometer. The standard calibration curves for each dye were measured as described earlier. Simultaneously, blank values were determined by using extraction systems without dyes to prevent cross-contamination from phase constituents. Every experiment was performed in duplicate to ensure accuracy in the results.

Equations 7−9 were employed to calculate the phase volume ratio (R_{dye}), partition coefficient (K_{dye}), and extraction efficiency (EE_{dye} %), respectively

$$R_{dye} = \frac{V_T}{V_B} \tag{7}$$

$$K_{dye} = \frac{C_T}{C_B} \tag{8}$$

$$EE_{dye}\ (\%) = \frac{C_T V_T}{C_T V_T + C_B V_B} \times 100 \tag{9}$$

where the volumes of the top phase and bottom phase are denoted by V_T and V_B, respectively. C_T and C_B represent the equilibrium dye concentrations in the top and bottom phases, respectively.

3. RESULTS AND DISCUSSION

3.1. Phase Diagrams. The information on the phase diagram for the investigated systems is most important for the extraction of desired compounds in separation science. The binodal curve gives relevant information about the weight fraction of DES, water, and salt required to obtain phase separation for DES-based ATPS. The data of binodal curves were collected at atmospheric pressure and 298.15 K.

The weight fraction data for binodal curves of DES-based ATPS; BTBAC:alcohols; and BTBAC:PEGs with K_3PO_4/K_2HPO_4/K_2CO_3 are given in Tables S4 to S9 as Supporting Information and graphically represented in Figure 3A−C for BTBAC:alcohols DESs and Figure 4A−C for BTBAC:PEG-based DESs. According to the electroneutrality in both phases, interactions between cations and anions of HBA and HBD were

https://doi.org/10.1021/acs.jced.5c00346
J. Chem. Eng. Data 2025, 70, 3364−3377

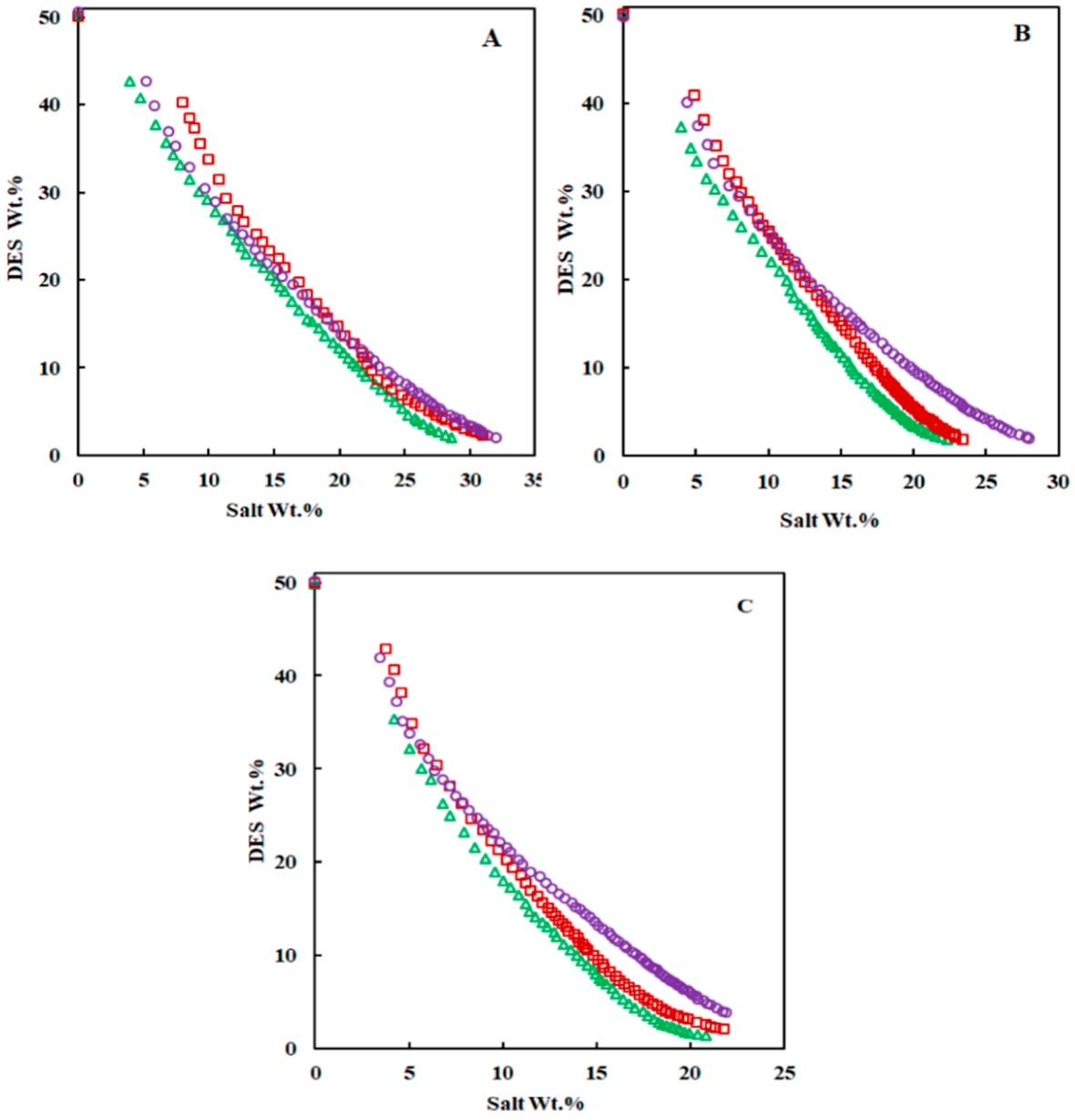

Figure 4. Effect of inorganic salts **green Δ: K_3PO_4 violet O: K_2HPO_4, red □: K_2CO_3** on the phase behavior of various DES:PEG-based ATPS at atmospheric pressure and 298.15 K. (A) BTBAC:PEG 200, (B) BTBAC:PEG 400, (C) BTBAC:PEG 600. The plots are drawn using data presented in Tables S7−S9.

observed in DES-based ATPS during the separation of phases.[45] The experimentally determined weight fraction values for the binodal curve provided a more accurate representation of ATP behavior when considering the concentration of salt than the concentration of individual ions.[46] Therefore, phase diagrams were plotted using the concentrations of salt and DES measured by the cloud point experiment.

3.1.1. Influence of Inorganic Salt on Phase Behavior. The influence of inorganic salts on ATPS formation was investigated for all DES systems specifically, BTBAC:alcohols and BTBAC:PEGs, which were prepared with K_3PO_4/K_2HPO_4/K_2CO_3. The capacity of inorganic salts to induce phase separation was observed as K_3PO_4 > K_2HPO_4 ≈ K_2CO_3 for the majority of studied ATPS, as shown in Figures 3 and 4A−C. BTBAC:PEG 600 containing DES showed the highest capacity of phase formation with K_3PO_4 followed by K_2HPO_4 or K_2CO_3, i.e., K_3PO_4 > K_2HPO_4 ≈ K_2CO_3 (Figures 3C and 4C). The salting-out pattern shown by the salts is based on their ability to salt out DES as per the Hofmeister series.[47] The binodal curves for K_2HPO_4 and K_2CO_3 were merged together at a lower salt concentration. However, both curves get separated as the salt concentration increases during the experiment.

The observed sequence of salts for salting-out capacity and merging of the curves can be accessed from the Gibbs free energy of hydration (ΔG_{hyd}) and molar entropy of hydration (ΔS_{hyd}) values of the anions. The salting-out ability of anions follows: PO_4^{3-} (ΔG_{hyd} = −2835 kJ·mol^{-1}, ΔS_{hyd} = −421 J·K^{-1}·mol^{-1}) > HPO_4^{2-} (ΔG_{hyd} = −1125 kJ·mol^{-1}, ΔS_{hyd} = −272 J·K^{-1}·mol^{-1}) > CO_3^{2-} (ΔG_{hyd} = −1300 kJ mol^{-1}, ΔS_{hyd} = −245 J·K^{-1}·mol^{-1}). As explained in the Hofmeister series, anions with greater valency and the highest negative ΔG_{hyd} values have more interactions with H_2O and are easily accessible to form ATP. It is also reported that H_2O molecules are more likely to link with inorganic salt as compared to DES during ATPS formation.[48]

https://doi.org/10.1021/acs.jced.5c00346
J. Chem. Eng. Data 2025, 70, 3364−3377

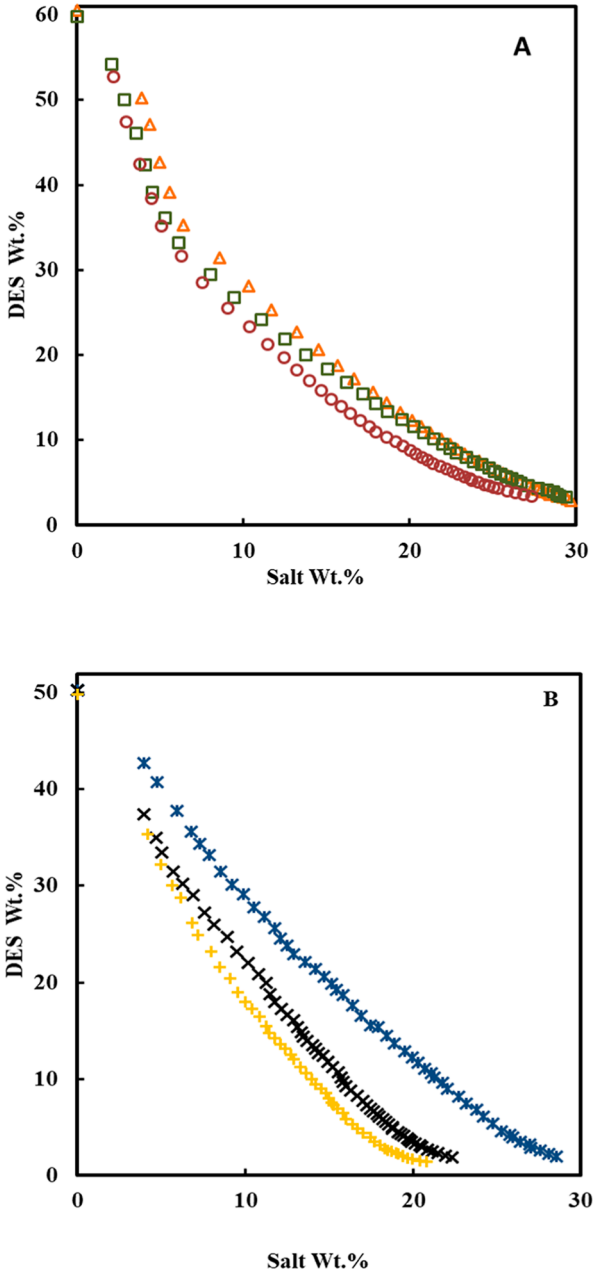

Figure 5. Effect of HBDs orange Δ: MEOH, red O: ETOH, green □: PROH, blue *: PEG 200, black x: PEG 400, and yellow +: PEG 600 on the phase behavior of (A) alcohol-based DESs, (B) PEG-based DESs with K_3PO_4 at 298.15 K and atmospheric pressure. The plots are drawn using data presented in Tables S4−S9 (only with K_3PO_4).

The main reason could be higher capacity of salts to create hydration complexes than DES, as per previously examined mechanism of DES-ATPS formation.[35,49] The main reason for the formation of DES:salt-based ATPS is the presence of hydration complexes between the high charge density salt and HBA (usually a quaternary ammonium salt). HBD acts as an additive to regulate the equilibrium between the properties of both phases. It can be concluded that the salting-out capacity of salts was observed as $K_3PO_4 > K_2HPO_4 \approx K_2CO_3$, corresponding to the order observed for anion of salt by the Hofmeister series and their corresponding ΔG_{hyd} and ΔS_{hyd} values. A similar observation was recorded for DES:salt-based ATPS in the literature.[47−49] Zafarani-Moattar[50] investigated the applicability of ATPS comprising ChCl:PEG-based DESs with K_3PO_4/K_2HPO_4 salts to extract amino acids (L-threonine and L-tryptophan). The extraction capacity of ATPS for the extraction of both amino acids was reported to be around 99.50%. The extraction of spirulina phycocyanin was studied by Zhuang et al.[51] using DES: salt-based ATPS ChCl−urea with K_2HPO_4 salt. The efficiency and yield of the extraction were 94.20% and 92.00%, respectively. Recently, hexafluoroisopropanol (HFIP)-based DES + K_2HPO_4 salt-based ATPS was developed by Yu et al.[52] to extract flavonoids from Flos Sophorae Immaturus (FSI). The extraction efficiency for flavonoid was 95.00%, and the FSI yield was 21.05%.

3.1.2. Influence of DES on Phase Behavior. The hydrophilic HBDs have been utilized to prepare DESs in this study. Thus, the discussion is necessary to explore the impact of HBDs of DESs on phase behavior. The effect of alcohol and PEG on phase behavior is depicted separately in Figure 5A,B, respectively, as the comparison of all six HBDs is not very pronounced and clear. According to Figure 5, the capacity of DESs to induce phase separation for all of the salts under investigation follows the order: BTBAC:PROH > BTBAC:ETOH > BTBAC:MEOH and BTBAC:PEG 600 > BTBAC:PEG 400 > BTBAC:PEG 200. Due to the higher hydrophobicity of HBD, DESs composed of PROH and PEG 600 showed the maximum phase-forming capacity. The log K_{ow} values (octanol−water partition coefficient) for MEOH, ETOH, and PROH are −0.63, −0.14, and 0.35, respectively. The large negative values of log K_{ow} reveal the least hydrophobic nature in comparison to PROH and ETOH. In case of PEGs, the least negative log K_{ow} value was reported for PEG 600, followed by PEG 400 and PEG 200.[53] A similar trend was observed during the ATPS study of benzyltriethylammonium chloride and benzyltrimethylammonium chloride with potassium salts.[34] The same observations were reported for phase separation for propanol containing DESs. They reported the maximum capacity of phase separation by *tert*-butanol-based DESs.[54] The increasing chain length in the structure of HBD leads to an increase in the hydrophobic nature and phase-inducing capacity of DESs. The obtained results of the binodal curves were explained in terms of the hydrophobicity of the HBDs for the investigated DESs. The effective excluded volume theory also explains the effect of alcohol on the formation of ATP.[55] The strength of molecular interactions in alcohol and PEG plays a critical role in the determination of the boiling temperature. PROH and PEG 600 have greater amount of hydrogen bonding, higher boiling point, and the capacity to form ATP as compared to MEOH/ETOH/PEG 200/PEG 400.

3.2. Partitioning of Dyes. The partitioning capability of ATPS was demonstrated using three dyes of varying polarities (MG, IB, and SIII) in order to consider the practical application of ATPS generated by alcohol and PEG-based DESs and inorganic salts. The effect of potassium salts and HBDs of DESs on the partitioning of dyes was examined entirely based on the phase equilibria results described above. For comparison of the experimental results, 40 wt % DES + 18 wt % salt + 42 wt % aqueous dye solution was used for the alcohol-DES based system, and 25 wt % DES + 9 wt % salt + 66 wt % aqueous dye solution was used for the PEG-DES systems to create the biphasic region at atmospheric pressure and 298.15 K. The calculated partition coefficients (K_{dyes}) and extraction efficiencies (EE_{dyes} %) are depicted in Figures 6A−C and S3A−C and Tables 2 and 3, respectively.

3.2.1. Influence of Potassium Salts on the Partitioning of Dyes. As reported previously, the potential of inorganic salts

https://doi.org/10.1021/acs.jced.5c00346
J. Chem. Eng. Data 2025, 70, 3364−3377

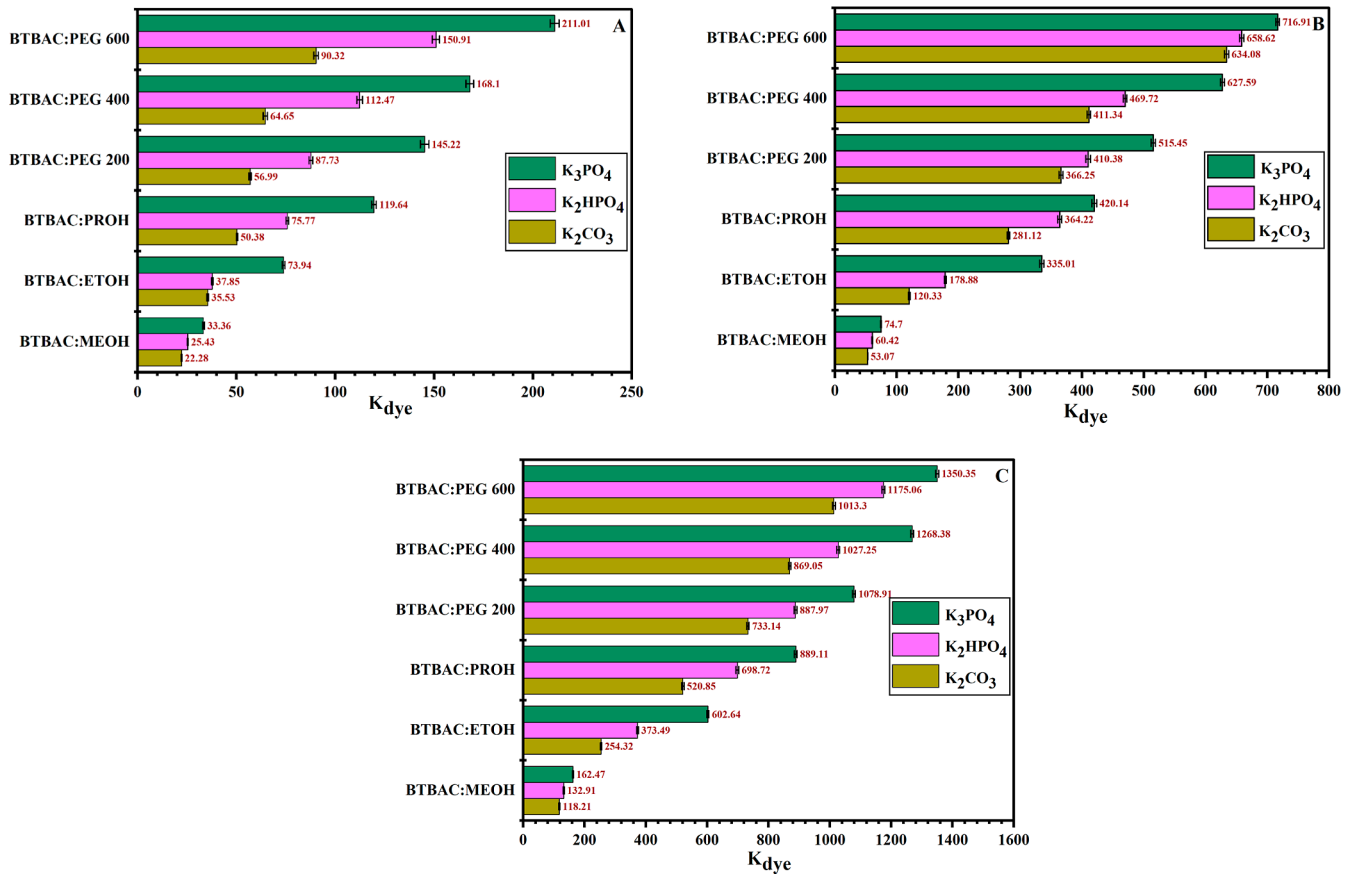

Figure 6. Partition coefficients (K_{dye}) of (A) MG, (B) IB, (C) SIII for investigated DES-based ATPS as presented in Table 2 at 298.15 K and atmospheric pressure.

Table 2. Partition Coefficients of Dyes (K_{dyes}) in Investigated DES-Based ATPS at 298.15 K and Atmospheric Pressure[a]

ATPS	salt	MG	IB	SIII
BTBAC:MEOH	K_2CO_3	22.28 ± 0.15	53.07 ± 0.34	118.21 ± 1.24
	K_2HPO_4	25.43 ± 0.24	60.42 ± 0.55	132.91 ± 1.67
	K_3PO_4	33.36 ± 0.52	74.7 ± 0.65	162.47 ± 1.85
BTBAC:ETOH	K_2CO_3	35.53 ± 0.45	120.33 + 1.54	254.32 ± 2.21
	K_2HPO_4	37.85 ± 0.35	178.88 ± 1.63	373.49 ± 2.85
	K_3PO_4	73.94 + 0.65	335.01 ± 3.35	602.64 ± 3.20
BTBAC:PROH	K_2CO_3	50.38 ± 0.35	281.12 + 1.95	520.85 ± 3.84
	K_2HPO_4	75.77 ± 0.65	364.22 ± 3.32	698.72 ± 4.52
	K_3PO_4	119.64 ± 1.12	420.14 ± 3.86	889.11 ± 4.21
BTBAC:PEG 200	K_2CO_3	56.99 ± 0.56	366.25 ± 3.27	733.14 ± 4.10
	K_2HPO_4	87.73 ± 0.95	410.38 ± 3.86	887.97 ± 4.65
	K_3PO_4	145.22 ± 2.17	515.45 ± 3.58	1078.91 ± 4.89
BTBAC:PEG 400	K_2CO_3	64.65 ± 1.05	411.34 ± 2.86	869.05 ± 3.95
	K_2HPO_4	112.47 ± 1.45	469.72 ± 2.89	1027.25 ± 4.32
	K_3PO_4	168.1 ± 1.95	627.59 ± 3.11	1268.38 ± 4.52
BTBAC:PEG 600	K_2CO_3	90.32 ± 1.12	634.08 ± 3.35	1013.3 ± 4.56
	K_2HPO_4	150.91 ± 1.83	658.62 ± 3.58	1175.06 ± 4.68
	K_3PO_4	211.01 + 2.27	716.91 ± 2.82	1350.35 ± 4.85

[a]The standard uncertainties (u) for temperature, pressure, and partitioning coefficient are $u(T)$ = ±0.05 K, $u(p)$ = ±0.5 kPa, and $u(K_{dye})$ = ±0.15, respectively.

(phase formers) to salt out DESs was observed in the following sequence for all ATPS studied: K_3PO_4 > K_2HPO_4 ≈ K_2CO_3. Specifically, the BTBAC:PEG 600 + K_2CO_3 system yielded K_{dye} value = 90.32 (Table 2) and EE_{dye} % = 97.99% (Table 3), whereas the BTBAC:PEG 600 + K_3PO_4 system gave a maximum K_{dye} = 211.01 (Table 2) and EE_{dye} % = 98.92% (Table 3) for MG dye. Almost all studied ATPS showed a similar trend in our study. Additionally, it was noted that the K_{dye} values recorded in each of the studied ATPS were greater than 1.

BTBAC:PEG 600 + K_3PO_4 ATPS showed higher K_{dye} and EE_{dye} % for all examined dyes (Tables 2 and 3). The study found that BTBAC:PEG 600 + K_3PO_4 showed the highest extraction

https://doi.org/10.1021/acs.jced.5c00346
J. Chem. Eng. Data 2025, 70, 3364−3377

Table 3. Extraction Efficiencies (EE_{dye} %) of Dyes in the Investigated DES-Based ATPS at 298.15 K and Atmospheric Pressure[a]

DESs	salt	MG	IB	SIII
BTBAC:MEOH	K_2CO_3	93.20 ± 1.25	97.70 ± 1.25	99.57 ± 1.28
	K_2HPO_4	94.61 ± 1.29	97.98 ± 1.35	99.68 ± 1.24
	K_3PO_4	95.87 + 1.33	98.57 ± 1.41	99.86 ± 1.39
BTBAC:ETOH	K_2CO_3	94.42 + 1.21	98.60 ± 1.26	99.91 ± 1.24
	K_2HPO_4	95.62 ± 1.38	98.69 ± 1.32	99.96 ± 1.33
	K_3PO_4	96.22 ± 1.35	98.99 ± 1.39	99.98 ± 1.45
BTBAC:PROH	K_2CO_3	96.12 ± 1.47	99.79 ± 1.53	99.99 ± 1.55
	K_2HPO_4	96.61 ± 1.52	99.84 ± 1.65	99.99 ± 1.65
	K_3PO_4	97.75 + 1.62	99.85 ± 1.72	100 ± 1.77
BTBAC:PEG 200	K_2CO_3	96.88 ± 1.87	99.88 ± 1.75	99.99 + 1.98
	K_2HPO_4	97.70 ± 2.46	99.92 ± 1.78	99.99 ± 1.75
	K_3PO_4	98.61 ± 1.93	99.95 ± 1.92	100 ± 1.98
BTBAC:PEG 400	K_2CO_3	97.68 ± 1.84	99.92 ± 1.75	99.99 ± 1.79
	K_2HPO_4	97.84 ± 1.92	99.95 ± 1.89	100 ± 1.85
	K_3PO_4	98.75 ± 2.63	99.97 ± 2.25	100 ± 2.56
BTBAC:PEG 600	K_2CO_3	97.99 ± 2.34	99.98 ± 2.05	100 ± 1.98
	K_2HPO_4	98.42 ± 1.92	99.99 ± 2.29	100 ± 1.89
	K_3PO_4	98.92 ± 2.68	100 ± 2.42	100 ± 2.22

[a]The standard uncertainties (u) for temperature, pressure, and extraction efficiency are $u(T) = \pm 0.05$ K, $u(p) = \pm 0.5$ kPa, and $u(EE_{dye}\ \%) = \pm 0.15$, respectively.

performance among the studied dyes due to its higher phase-forming ability and higher hydrophobicity as compared to the other ATPS under investigation. All dyes preferred the hydrophobic DES-rich top phase for their hydrophobic nature over the hydrophilic salt-rich bottom phase.

In other words, all of the dyes under study readily interacted via intermolecular hydrogen bonds with DES and water, forcing them to concentrate in the hydrophobic phase. As shown in Figures 6 and S3A−C, K_{dyes} and EE_{dye} % of BTBAC:alcohol and PEG-based systems decrease with a decrease in the phase-forming capability of the salts. The dye could not transfer to the DES-rich top phase due to the lowest salting-out capacity of salt and least phase separation in ATPS.[56]

3.2.2. Influence of DESs on Partitioning of Dyes. The study also examined the impact of HBDs of DESs on the partitioning behavior of dyes in the investigated ATPS. BTBAC:MEOH-based ATPS showed the lowest K_{dyes} and EE_{dye} % values, whereas systems based on BTBAC:PEG 600 APTS resulted in the highest K_{dyes} and EE_{dye} % values for all examined dyes, as shown in Figures 7A,B and 8A,B. According to the research, the HBDs partitioning ability follows trends according to their log K_{ow} values: PROH ($\log K_{ow} = 0.35$) > ETOH ($\log K_{ow} = -0.14$) > MEOH ($\log K_{ow} = -0.65$).

The observed pattern is related to the hydrophobicity of the relevant HBDs. The most hydrophobic DESs interacted strongly with hydrophobic dyes. Additionally, the study found that increasing the molecular weight of HBD (PEGs from 200 to 600) improved the hydrophobicity of the corresponding DES.[23] The BTBAC:PEG 600 and K_3PO_4 system showed highest extraction efficiencies for the three dyes studied due to higher hydrophobicity of the system through maximum molar mass of HBD and salt (K_3PO_4) with maximum salting-out capacity as compared to the other systems investigated. Consequently, it can be summarized that the HBDs of DESs under investigation were extremely important in partitioning behavior of compounds of interest.

3.2.3. Influence of Hydrophobicity of Dyes. The octanol−water partition coefficient ($\log K_{ow}$) value for each dye examined is positive (i.e., hydrophobic character), therefore easily partitioned in the top phase containing hydrophobic DES. Figures 7A,B and 8A,B demonstrate that the extraction efficiency decreases with a decrease in log $K_{ow}$of the investigated dyes. The log K_{ow} values for dyes decrease as SIII (7.47) > IB (2.65) > MG (0.62).[57−59] A greater value of log K_{ow} indicates that the dye has a better chance of migrating into the higher hydrophobic component containing phase.[60] SIII and IB are more hydrophobic in nature due to more aromatic functional groups in their chemical structure than MG. The hydrophobicity of the dyes under investigation is evident from their structural variance and log K_{ow} values. The structure of the dye and its hydrophobic interactions with the constituents of the DES system usually determine preference during the extraction process.

The values of K_{dye} (Figures 7A and 8A) and EE_{dye} % (Figures 7B and 8B) were lowest for MG in all investigated ATPS. Interestingly, all studied ATPS resulted in the highest K_{dye} (Figures 7A and 8A) and EE_{dye} % values (Figures 7B and 8B) for SIII. For all studied ATPS, K_{dye} and EE_{dye} % values for all dyes follow the order: SIII > IB > MG. The nonpolar groups present in dyes reduce their attraction with water and enhance transfer toward the DES-rich top phase. For ATPS composed of BTBAC:PEG 600 with K_3PO_4, the K_{dye} values were calculated around 1350.35, 716.90, and 211.01 for SIII, IB, and MG, respectively (Table 2 and Figure 8A), and EE_{dye} % for SIII, IB, and MG using the same extraction technique was found around 100%, 100%, and 98.92%, respectively (Table 3 and Figure 8B). BTBAC:PEG 400 + K_3PO_4 and BTBAC:PEG 600 + K_3PO_4 ATPS showed the complete extraction of SIII and IB dyes. DES-based ATPS have been studied for the extraction of methylene blue, methyl orange, congo red,[32] methyl orange, eriochrome black T, and eosin Y.[35] The extraction efficiency of these dyes was closely associated with their log K_{ow}/hydrophobicity. A recent study used biomolecules and dyes to examine the extraction capability of polypropylene glycol (PPG)−quaternary ammonium salt-based ATPS. The K_{dye} values for methylene blue, caffeine, codeine, vanillin, curcumin, rhodamine, and Sudan III were 2.23, 4.50, 8.85, 20.52, 407.93, 174.91, and 1350.74, respectively. The highest EE_{dye} % around

https://doi.org/10.1021/acs.jced.5c00346
J. Chem. Eng. Data 2025, 70, 3364−3377

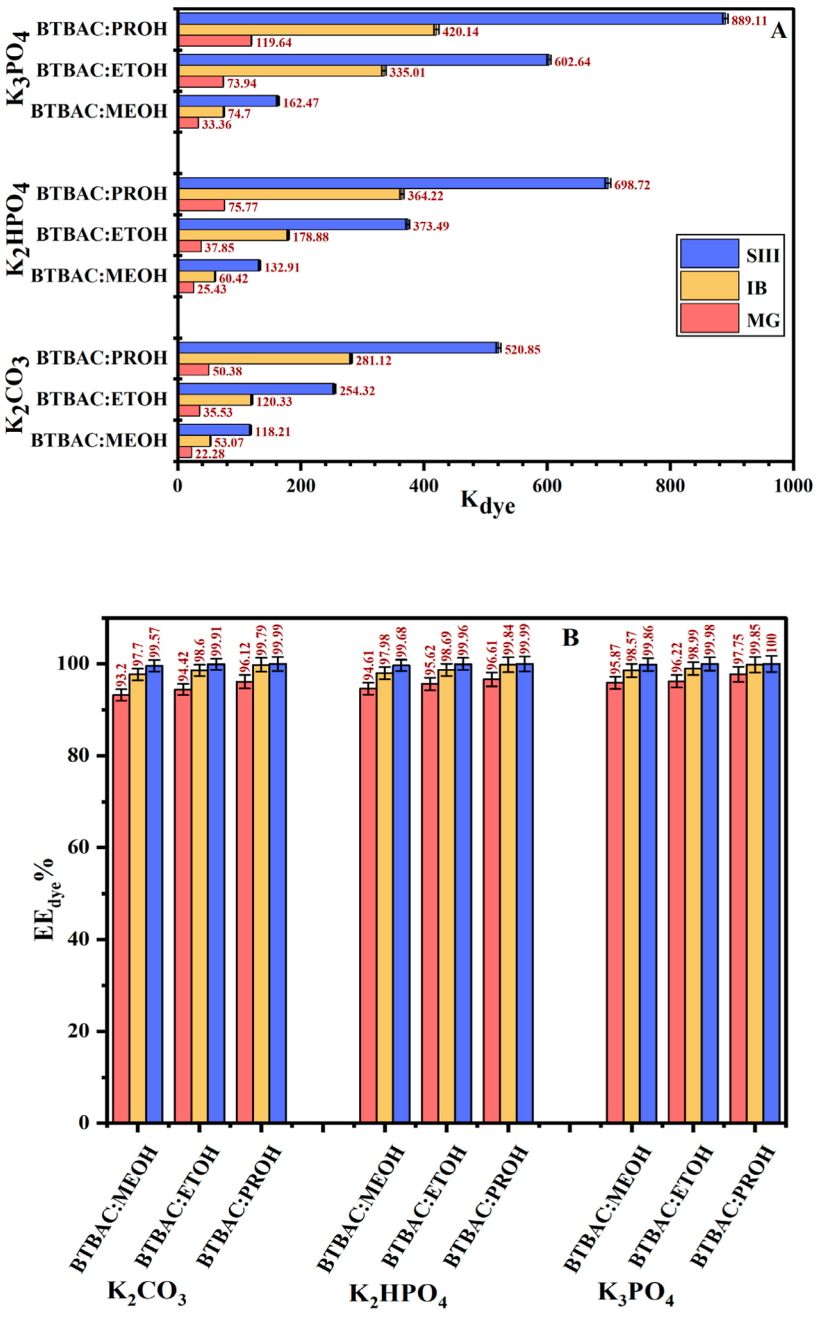

Figure 7. Effect of HBDs of various alcohol-based DESs: (A) partition coefficient (K_{dyes}) and (B) extraction efficiency (EE_{dyes} %) (pink-MG, orange-IB, and blue-SIII) of BTBAC-based ATPS at 298.15 K and atmospheric pressure (Tables 2 and 3).

100%, 98.80%, and 95.80% was reported for Sudan III, rhodamine B, and methylene blue, respectively.[56]

3.3. Comparison with Other Types of ATPS Available in the Literature. Table 4 presents a comparison of extraction efficiency (EE_{dye} %) of the studied ATPS with ATPS reported in the literature for the extraction of the reported dye in the present investigation. The studied ATPS and majority of reported systems either with polymer or ILs or DESs showed 100% extraction of dyes, except ATP composed of polymerized DES and inorganic salt reported around 95.00%−98.00% efficiency for Sudan III,[57,67] and polymer-salt systems[50,59,60,68,69] have reported around >97.00% for all the dyes as reported in Table 4 except for sunset yellow and methyl orange, it was found around 76.00.[66,67] The comparison results show that the presently investigated ATPS can also be considered as a potential system for 100% extraction of textile dyes.

4. CONCLUSIONS

This MS report reports six new DESs composed of benzyltributylammonium chloride and different HBDs: MEOH, ETOH, PROH, PEG 200, PEG 400, and PEG 600. The ATPS were designed at 298.15 K with atmospheric pressure using BTBAC-based DESs with potassium salts. The studied ATPS were investigated in terms of the characteristics of salt and HBD. The effect of the nature of salt and HBD on the formulation of ATPS was investigated. The obtained results showed that both have a profound effect on the position of the binodal curve in the phase equilibria of the studied systems. The salting-out ability of salts was reported in the sequence of K_3PO_4

https://doi.org/10.1021/acs.jced.5c00346
J. Chem. Eng. Data 2025, 70, 3364−3377

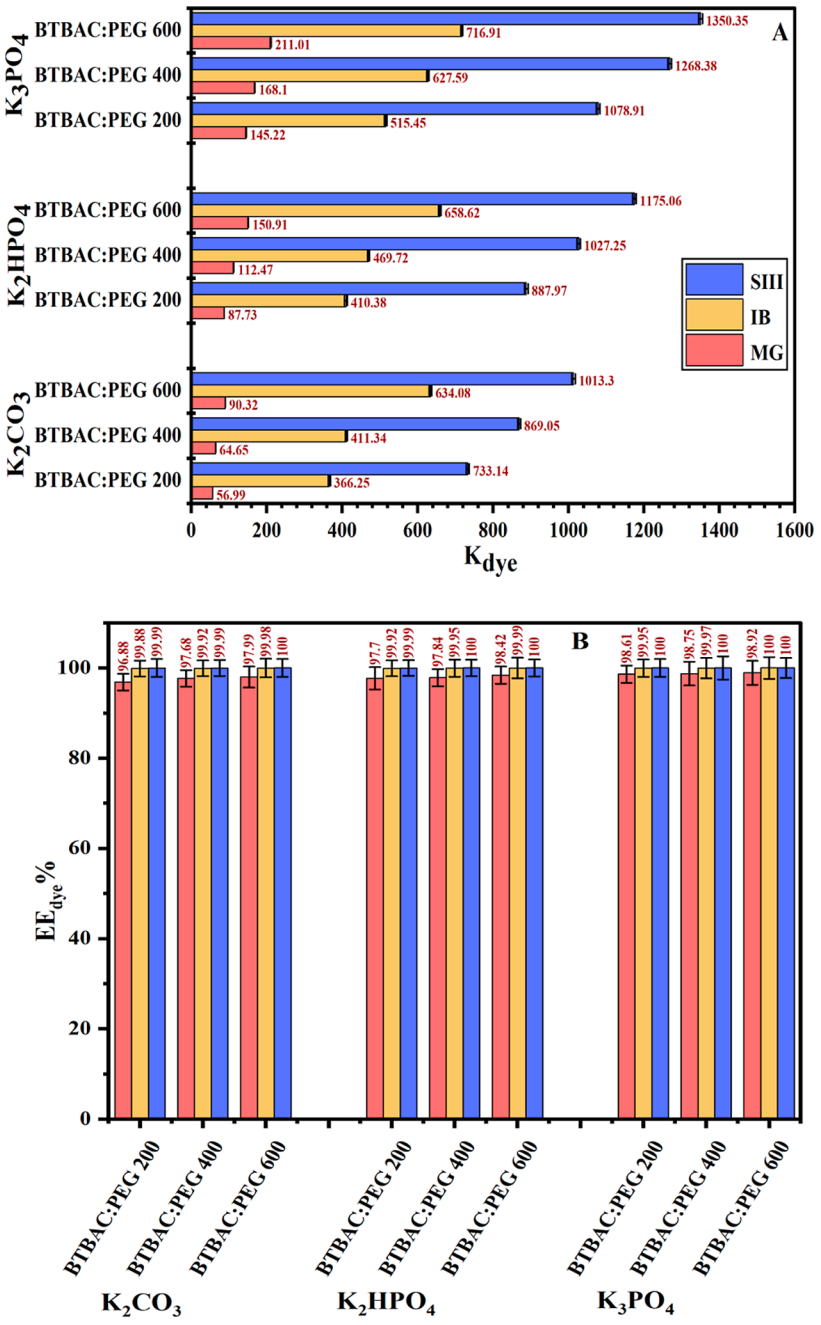

Figure 8. Effect of HBDs of various polymer-based DESs: (A) partition coefficient (K_{dyes}) and (B) extraction efficiency (EE_{dyes} %) (pink-MG, orange-IB, and blue-SIII) of BTBAC-based ATPS at 298.15 K and atmospheric pressure (Tables 2 and 3).

> $K_2HPO_4 \approx K_2CO_3$. The applicability of ATPS was tested for the extraction of three dyes: MG, IB, and SIII. The roles of salt, DES components, and dye hydrophobicity were carefully assessed. The salting-out capacity of salts, alkyl chain length of HBA and HBD in DESs, and hydrophobic characteristics of dyes play important roles in finding the extraction efficiency of the developed ATPS. BTBAC:PEG 600 and K_3PO_4 ATPS achieved complete extraction (100%) of all three dyes examined. In general, the DES-based ATPS explored in this investigation showed an excellent capacity to extract a wide range of dyes, irrespective of their complex structures or physicochemical properties.

■ ASSOCIATED CONTENT

Supporting Information

The Supporting Information is available free of charge at https://pubs.acs.org/doi/10.1021/acs.jced.5c00346.

Chemical name, acronym, source, CAS number, and purity of the chemicals; experimental binodal mass fraction data for systems composed of PEG + salts + H_2O and BTBAC:alcohol/PEG + salts + H_2O; correlation parameters of eq 1 and R^2 of the binodal curves for the investigated DES-based ATPS at 298.15 K and atmospheric pressure; chemical structures of dyes; comparison of phase behavior of various PEG-based ATPS; and extraction efficiencies of dyes in various alcohol and polymer-based DESs ATPS (PDF)

https://doi.org/10.1021/acs.jced.5c00346
J. Chem. Eng. Data 2025, 70, 3364−3377

Table 4. Comparison of the Obtained Results with Different Types of ATPS Reported in the Literature at 298.15 K[a]

type of ATPS	component 1 of ATPS	component 2 of ATPS	dyes	EE_{dye} %	ref
DES/salt	BTEAC:PROH	K_3PO_4	alizarin red S	98.20	34
			orange II	99.13	
			congo red	99.61	
DES/salt	BTBAC:TEG	K_3PO_4, K_2HPO_4	eosin Y, eriochrome black T, methyl orange	100	35
IL/salt	$[P_{4444}]Br$, $[P_{4441}][CH_3SO_4]$, $[P_{4444}]Cl$	$K_3C_6H_5O_7$	Sudan III, indigo blue	100	61
polymer/IL	PPG 400	[N111(2OH)]Cl, [N111(2OH)]Ace, [N111(2OH)Glyl, [N111(2OH)Lacl, [N111(2OH)]DHC	Sudan III	100	29
DES/DES	TBAB:PPG 400	ChCl:glycerol	Sudan III	94.87	31
DES/salt polymer/salt	TBAB:PPG 400, PPG 400	Na_2CO_3	Sudan III	98.00	56
DES/polymer DES/salt	BTMAC:glycerin	PPG 1000, K_2HPO_4	Sudan III	98.47	28
polymer/salt	PPG 400	TMAC	Sudan III	100	57
	PEO 1500, PEO 400	$Na_2C_4H_4O_6$, Na_2SO_4	malachite green	97.95, 97.50	62
	PEG 1500	$(NH_4)_2SO_4$	remazol golden yellow, methylene blue	>97.00	63
	PEG 1500	$Na_3C_6H_5O_7$	acid blue 9	98.85	64
	PEG 6000	Na_2CO_3	cibacron scarlet LS 2G, brown ERN, astacryl red 3B, rhodamine B	>98.00	65
	PEG 600	Na_2SO_4	sunset yellow FCF	76.50	66
	PEG 400	Na_2SO_4	methyl orange	73.27	67
	PEG 2000	K_2CO_3	remazol brilliant blue R, congo red	>99.00	60
	PEG 1500	Li_2SO_4	remazol yellow gold RNL	≈100	68
	PPG 400	Na_2CO_3	amaranth	>95.00	55
	PPG 400	$K_3C_6H_5O_7$	methyl orange	97.80	32
			methylene blue	94.00	
			congo red	>99.00	
	PEG 4000	Na_2CO_3	brilliant blue FCF	>96.00	69
DES/salt	BTBAC:PEG 600	K_3PO_4	malachite green	98.92	this work
			indigo blue	100	
			Sudan III	100	

[a]$[P_{4444}]Br$—tetrabutylphosphonium bromide; $[P_{4441}][CH_3SO_4]$—tributylmethylphosphonium methyl sulfate; $[P_{4444}]Cl$—tetrabutylphosphonium chloride; [N111(2OH)]Cl—cholinium chloride; [N111(2OH)]Ace—cholinium acetate; [N111(2OH)]Glyl—cholinium glycolate; [N111-(2OH)]Lacl—cholinium lactate; [N111(2OH)]DHC—cholinium dihydrogen citrate; TMAC—tetramethylammonium chloride; TBAB—tetrabutylammonium bromide; BTMAC—benzyltrimethylammonium chloride; $K_3C_6H_5O_7$—potassium citrate; $Na_2C_4H_4O_6$—sodium tartrate; Na_2CO_3—sodium carbonate; PPG—polypropylene glycol; PEO—poly(ethylene oxide).

AUTHOR INFORMATION

Corresponding Author

Sushma P. Ijardar − *Department of Chemistry, Veer Narmad South Gujarat University, 395007 Surat, India;* orcid.org/0000-0001-9079-0701; Email: sijardar@vnsgu.ac.in

Authors

Nensi A. Patel − *Department of Chemistry, Veer Narmad South Gujarat University, 395007 Surat, India*

Emmanuel A. Oke − *Department of Chemistry, Veer Narmad South Gujarat University, 395007 Surat, India; School of Chemical and Metallurgical Engineering, University of the Witwatersrand Johannesburg, 2050 Johannesburg, South Africa;* orcid.org/0000-0001-5774-6215

Complete contact information is available at: https://pubs.acs.org/10.1021/acs.jced.5c00346

Author Contributions

Nensi A. Patel: acquisition of data, analysis and interpretation of data, and writing—original draft of manuscript. Emmanuel A. Oke: acquisition of data, data curation, and writing—original draft of manuscript. Sushma P. Ijardar: concept of original study, supervision, project administration, review, and editing.

Notes

The authors declare no competing financial interest.

ACKNOWLEDGMENTS

N.A.P. acknowledges the SHODH fellowship (reference no. 2022017497) by the Government of Gujarat, India. S.P.I. is grateful for the financial support provided by Veer Narmad South Gujarat University (UGC/17158), Surat, Gujarat, India and UGC DAE CSR 2021-22 (CRS/2021-22/03/566) to complete this study.

REFERENCES

(1) Li, M.; Han, N.; Zhang, X.; Wang, S.; Jiang, M.; Bokhari, A.; Zhang, W.; Race, M.; Shen, Z.; Chen, R.; Mubashir, M.; Khoo, K. S.; Teo, S. S.; Show, P. L. Perovskite oxide for emerging photo(electro)-catalysis in energy and environment. *Environ. Res.* **2022**, *205*, 112544.

(2) Oke, E. A.; Ijardar, S. P. Insights into the separation of metals, dyes and pesticides using ionic liquid based aqueous biphasic systems. *J. Mol. Liq.* **2021**, *334*, 116027.

(3) Oke, E. A.; Sharma, R.; Malek, N. I.; Ijardar, S. P. Applications of deep eutectic solvents in remediation of emerging contaminants. In *Current Developments in Biotechnology and Bioengineering*; Elsevier, 2022; pp 223−246.

(4) Dutta, S.; Adhikary, S.; Bhattacharya, S.; Roy, D.; Chatterjee, S.; Chakraborty, A.; Banerjee, D.; Ganguly, A.; Nanda, S.; Rajak, P. Contamination of textile dyes in aquatic environment: Adverse impacts on aquatic ecosystem and human health, and its management using bioremediation. *J. Environ. Manage.* **2024**, *353*, 120103.
(5) Al-Tohamy, R.; Ali, S. S.; Li, F.; Okasha, K. M.; Mahmoud, Y. A. G.; Elsamahy, T.; Jiao, H.; Fu, Y.; Sun, J. A critical review on the treatment of dye-containing wastewater: Ecotoxicological and health concerns of textile dyes and possible remediation approaches for environmental safety. *Ecotoxicol. Environ. Saf.* **2022**, *231*, 113160.
(6) Lellis, B.; Fávaro-Polonio, C. Z.; Pamphile, J. A.; Polonio, J. C. Effects of textile dyes on health and the environment and bioremediation potential of living organisms. *Biotechnol. Res. Innov.* **2019**, *3*, 275−290.
(7) Benkhaya, S.; rabet, S. M.; El Harfi, A. A review on classifications, recent synthesis and applications of textile dyes. *Inorg. Chem. Commun.* **2020**, *115*, 107891.
(8) Sharma, J.; Sharma, S.; Soni, V. Classification and impact of synthetic textile dyes on aquatic Flora: a review. *Reg. Stud. Mar. Sci.* **2021**, *45*, 101802.
(9) Zahmatkesh, S.; Bokhari, A.; Karimian, M.; Zahra, M. M. A.; Sillanpää, M.; Panchal, H.; Alrubaie, A. J.; Rezakhani, Y. A comprehensive review of various approaches for treatment of tertiary wastewater with emerging contaminants: what do we know? *Environ. Monit. Assess.* **2022**, *194*, 884.
(10) Azanaw, A.; Birlie, B.; Teshome, B.; Jemberie, M. Textile effluent treatment methods and eco-friendly resolution of textile wastewater. *Case Stud. Chem. Environ. Eng.* **2022**, *6*, 100230.
(11) Nasrullah, A.; Bhat, A. H.; Naeem, A.; Isa, M. H.; Danish, M. High surface area mesoporous activated carbon-alginate beads for efficient removal of methylene blue. *Int. J. Biol. Macromol.* **2018**, *107*, 1792−1799.
(12) Jorge, A. M. S.; Athira, K. K.; Alves, M. B.; Gardas, R. L.; Pereira, J. F. B. Textile dyes effluents: A current scenario and the use of aqueous biphasic systems for the recovery of dyes. *J. Water Process Eng.* **2023**, *55*, 104125.
(13) Oke, E. A.; Ijardar, S. P. Advances in the application of deep eutectic solvents based aqueous biphasic systems: An up-to-date review. *Biochem. Eng. J.* **2021**, *176*, 108211.
(14) Ventura, S. P. M.; e Silva, F. A.; Quental, M. V.; Mondal, D.; Freire, M. G.; Coutinho, J. A. P. Ionic-Liquid-Mediated Extraction and Separation Processes for Bioactive Compounds: Past, Present, and Future Trends. *Chem. Rev.* **2017**, *117*, 6984−7052.
(15) Oke, E. A.; Ijardar, S. P. Partitioning behavior of dyes in ionic liquids induced aqueous biphasic systems of PPG 725 & ammonium salts. *Sep. Sci. Technol.* **2023**, *58*, 2463−2481.
(16) Ventura, S. P. M.; Coutinho, J. A. P. Toward the Recovery and Reuse of the ABS Phase-Forming Components. In *Ionic-Liquid-Based Aqueous Biphasic Systems*; Springer, Berlin, Heidelberg, 2016; pp 285−315.
(17) Patel, N. A.; Katrak, V. K.; Ijardar, S. P. Envisioning the applicability of stimuli responsive aqueous biphasic systems in the separation technology. *J. Mol. Liq.* **2025**, *423*, 127010.
(18) Marchel, M.; Coroadinha, A. S.; Marrucho, I. M. Novel Acidic Deep Eutectic Solvent-Based Aqueous Biphasic Systems for Efficient Extraction of Pepsin. *ACS Sustain. Chem. Eng.* **2020**, *8*, 12400−12408.
(19) Zhu, G.; Ren, B.; Zhou, Q.; Xiong, J.; Ma, X.; Zhao, L.; Jiang, F.; Yang, X.; Wang, S. Outstanding Performance of the Deep Eutectic Solvent-Based Aqueous Biphasic System Constructed with Sodium Citrate for a Green Gold Separation. *Langmuir* **2023**, *39* (27), 9538−9550.
(20) Singh, M. B.; Kumar, V. S.; Chaudhary, M.; Singh, P. A mini review on synthesis, properties and applications of deep eutectic solvents. *J. Indian Chem. Soc.* **2021**, *98*, 100210.
(21) Ramón, D. J.; Guillena, G. *Deep Eutectic Solvents*; Wiley, 2019.
(22) Ijardar, S. P.; Singh, V.; Gardas, R. L. Revisiting the Physicochemical Properties and Applications of Deep Eutectic Solvents. *Molecules* **2022**, *27*, 1368.
(23) Zhao, R.; Pei, D.; Yu, P.; Wei, J.; Wang, N.; Di, D.; Liu, Y. Aqueous two-phase systems based on deep eutectic solvents and their application in green separation processes. *J. Sep. Sci.* **2020**, *43*, 348−359.
(24) Zeng, Q.; Wang, Y.; Huang, Y.; Ding, X.; Chen, J.; Xu, K. Deep eutectic solvents as novel extraction media for protein partitioning. *Analyst* **2014**, *139*, 2565−2573.
(25) Farias, F. O.; Passos, H.; Lima, A. S.; Mafra, M. R.; Coutinho, J. A. P. Is it possible to create ternary-like aqueous biphasic systems with deep eutectic solvents? *ACS Sustain. Chem. Eng.* **2017**, *5*, 9402−9411.
(26) Yin, K.; Chen, L.; Liu, F.; Fan, T.; Wu, Y.; Li, S.; Yan, Z. Liquid-Liquid Equilibrium Data for Novel Aqueous Two-Phase Systems Composed of Betaine-Xylitol Deep Eutectic Solvent + Alcohol (1-Propanol/2-Propanol/tert-Butanol) + Water. *J. Chem. Eng. Data* **2022**, *67*, 2475−2485.
(27) Li, R.; Kang, K.; Li, J.; Wang, S.; Hang, F. Sustainable aqueous biphasic system created using sugar-based deep eutectic solvents/ethyl lactate for the green extraction of biomolecules. *J. Mol. Liq.* **2024**, *399*, 124474.
(28) Xu, K.; Zhao, Y.; Chen, K.; Dong, H.; Sun, S.; Ni, Z.; wang, Y. Aqueous biphasic systems developed with deep eutectic solvents and polymer for the efficient extraction of pigments from beverages. *Food Chem.* **2024**, *449*, 139206.
(29) Passos, H.; Tavares, D. J. P.; Ferreira, A. M.; Freire, M. G.; Coutinho, J. A. P. Are aqueous biphasic systems composed of deep eutectic solvents ternary or quaternary systems? *ACS Sustainable Chem. Eng.* **2016**, *4*, 2881−2886.
(30) Chen, J.; Wang, Y.; Wei, X.; Xu, W.; Xu, P.; Ni, R.; Meng, J. First investigation of the micelles forming in a novel deep eutectic solvents-based aqueous micellar two-phase system: partitioning of cationic/neutral/anionic pigments. *ACS Sustainable Chem. Eng.* **2019**, *7* (6), 6078−6092.
(31) Xu, K.; Xu, P.; Wang, Y. Aqueous biphasic systems formed by hydrophilic and hydrophobic deep eutectic solvents for the partitioning of dyes. *Talanta* **2020**, *213*, 120839.
(32) Zafarani-Moattar, M. T.; Shekaari, H.; Fattah, S. G.; Mokhtarpour, M. Novel aqueous twophase systems containing polymer-based deep eutectic solvent and citrate salts for high-performance extraction of dyes. *J. Mol. Liq.* **2022**, *360*, 119475.
(33) Basaiahgari, A.; Panda, S.; Gardas, R. L. Effect of Ethylene, Diethylene, and Triethylene Glycols and Glycerol on the Physicochemical Properties and Phase Behavior of Benzyltrimethyl and Benzyltributylammonium Chloride Based Deep Eutectic Solvents at 283.15−343.15 K. *J. Chem. Eng. Data* **2018**, *63*, 2613−2627.
(34) Oke, E. A.; Ijardar, S. P. Aqueous biphasic systems composed of alcohol-based deep eutectic solvents and inorganic salts: Application in the extraction of dyes with varying hydrophobicity. *J. Mol. Liq.* **2023**, *375*, 121372.
(35) Oke, E. A.; Ijardar, S. P. Insights into application of aqueous biphasic systems of deep eutectic solvents composed of benzyl tri alkylammonium chloride in dye separation. *Dyes Pigm.* **2024**, *224*, 112047.
(36) Asla, A.; Martínez-Rico, O.; Otero, P.; Domínguez, A.; Gonzalez, B. Water decolorization using tuned ternary Deep Eutectic solvents. *J. Mol. Liq.* **2023**, *381*, 121832.
(37) Martínez-Rico, O.; Asla, A.; Domínguez, A.; Gonzalez, B. Reversible dye extraction from aqueous matrices using ammonium salt-based deep eutectic solvents. *Sep. Purif. Technol.* **2024**, *335*, 126208.
(38) Tesfaye, B.; Gure, A.; Asere, T. G.; Molole, G. J. Deep eutectic solvent-based dispersive liquid-liquid microextraction for determination of organochlorine pesticides in water and apple juice samples. *Microchem. J.* **2023**, *195*, 109428.
(39) Bintanel-Cenis, J.; Fernandez, M. A.; Gomara, B.; Ramos, L. Critical overview on the use of hydrophobic (deep) eutectic solvents for the extraction of organic pollutants in complex matrices. *Talanta* **2024**, *270*, 125599.
(40) Wazeer, I.; Hizaddin, H. F.; El blidi, L.; Mulyono, S.; Hashim, M. A.; Hadj-Kali, M. K. Removal of cresol contaminants from aqueous

https://doi.org/10.1021/acs.jced.5c00346
J. Chem. Eng. Data 2025, 70, 3364−3377

media using hydrophobic deep eutectic solvents. *J. Mol. Liq.* **2024**, *407*, 125082.
(41) Gao, Z.; Jia, Z.; Liu, F.; Yang, L.; Cheng, Q.; Zhao, T. Hydrophobic deep eutectic solvents: Towards a greener and more efficient extraction process of Cr(VI) from aqueous solutions. *J. Environ. Chem. Eng.* **2025**, *13*, 115122.
(42) Mai, Y.; Xie, K.; Liang, S.; Li, G.; song, J.; Shi, C.; Song, Z.; Lin, X. Efficient extraction of 5-hydroxymethylfurfural from multi components aqueous solution by hydrophobic deep eutectic solvents. *Sep. Purif. Technol.* **2025**, *359*, 130572.
(43) Ghaedi, H.; Ayoub, M.; Sufian, S.; Lal, B.; Uemura, Y. Thermal stability and FT-IR analysis of Phosphonium-based deep eutectic solvents with different hydrogen bond donors. *J. Mol. Liq.* **2017**, *242*, 395−403.
(44) Merchuk, J. C.; Andrews, B. A.; Asenjo, J. A. Aqueous two-phase systems for protein separation Studies on phase inversion. *J. Chromatogr. B* **1998**, *711*, 285−293.
(45) Zhao, R. T.; Pei, D.; Yu, P. L.; Wei, J. T.; Wang, N. L.; Di, D. L.; Liu, Y. W. Aqueous two-phase systems based on deep eutectic solvents and their application in green separation processes. *J. Sep. Sci.* **2020**, *43*, 348−359.
(46) Bridges, N. J.; Gutowski, K. E.; Rogers, R. D. Investigation of aqueous biphasic systems formed from solutions of chaotropic salts with kosmotropic salts (salt-salt ABS). *Green Chem.* **2007**, *9* (2), 177−183.
(47) Shahriari, S.; Neves, C. M. S. S.; Freire, M. G.; Coutinho, J. A. P. Role of the Hofmeister series in the formation of ionic-liquid-based aqueous biphasic systems. *J. Phys. Chem. B* **2012**, *116*, 7252−7258.
(48) Li, N.; Wang, Y.; Xu, K.; Huang, Y.; Wen, Q.; Ding, X. Development of green betaine-based deep eutectic solvent aqueous two-phase system for the extraction of protein. *Talanta* **2016**, *152*, 23−32.
(49) Farias, F. O.; Passos, H.; Sanglard, M. G.; Igarashi-Mafra, L.; Coutinho, J. A. P.; Mafra, M. R. Designer solvent ability of alcohols in aqueous biphasic systems composed of deep eutectic solvents and potassium phosphate. *Sep. Purif. Technol.* **2018**, *200*, 84−93.
(50) Zafarani-Moattar, M. T.; Shekaari, H.; Ardi-Samberan, P. Thermodynamic Studies of L-tryptophan and L-threonine partitioning in aqueous two-phase systems containing deep eutectic solvents (choline chloride/PEG) and potassium salts. *J. Chem. Eng. Data* **2022**, *67* (5), 1214−1227.
(51) Zhuang, D.; Chew, K. W.; Teoh, W. Y.; Al-Maari, M. A. S.; Hizaddin, H. F.; Alharthi, S.; Show, P. L.; Ling, T. C. Extraction of phycocyanin from Spirulina using Deep Eutectic Solvent Liquid Biphasic System. *J. Taiwan Inst. Chem. Eng.* **2023**, *151*, 105125.
(52) Yu, J.; Wang, W.; Pan, X.; Wang, H.; Lang, Y.; Zhylko, V.; Wang, X.; Dai, L. Hexafluoroisopropanol-based deep eutectic solvents for efficient aqueous two-phase extraction of flavonoids from Flos Sophorae Immaturus. *Sep. Purif. Technol.* **2025**, *358*, 130216.
(53) USEPA. *Estimation Programs Interface Suite for Microsoft Windows, V 1.68*; United States Environmental Protection Agency: Washington, DC, USA, 2010.
(54) Sanglard, M. G.; Farias, F. O.; Sosa, F. H. B.; dos Santos, T. P. M.; Igarashi-Mafra, L.; Mafra, M. R. Measurement and correlation of aqueous biphasic systems composed of alcohol (1-propanol/2-propanol/tert-butanol) + $(NH_4)_2SO_4$ + H_2O at 298 K and a textile dye partition. *Fluid Phase Equilib.* **2018**, *466*, 7−13.
(55) Wang, Y.; Yan, Y.; Hu, S.; Han, J.; Xu, X. Phase diagrams of ammonium sulfate + ethanol/1-propanol/2-propanol + water aqueous two-phase systems at 298.15 K and correlation. *J. Chem. Eng. Data* **2010**, *55*, 876−881.
(56) Zhang, H.; Wang, Y.; Zhou, Y.; Chen, J.; Wei, X.; Xu, P. Aqueous biphasic systems formed by deep eutectic solvent and new-type salts for the high-performance extraction of pigments. *Talanta* **2018**, *181*, 210−216.
(57) Nosratpour, N.; Sadeghi, R.; Ebrahimi, N. Aqueous biphasic systems composed of polypropylene glycol and tetraalkylammonium salts: Thermodynamic investigation and application for efficient extraction of biomolecules and dyes. *J. Mol. Liq.* **2025**, *422*, 126964.
(58) *Chemspider, the Free Chemical Database*, 2013.
(59) Zhong, Y.; Wang, K.; Guo, C.; Kou, Y.; Hassan, A.; Lu, Y.; Wang, J.; Wang, W. Competition adsorption of malachite green and rhodamine B on polyethylene and polyvinyl chloride microplastics in aqueous environment. *Water Sci. Technol.* **2022**, *86* (5), 894−908.
(60) Jocić, A.; Marić, S.; Dimitrijević, A.; Tot, A.; Gadžurić, S.; Vraneš, M.; Trtić-Petrović, T. Protic ionic liquids as adjuvants to enhance extraction and separation performance of diverse polarity compounds in PEG-salt based aqueous biphasic system. *J. Mol. Liq.* **2020**, *303*, 112484.
(61) Ferreira, A. M.; Coutinho, J. A.; Fernandes, A. M.; Freire, M. G. Complete removal of textile dyes from aqueous media using ionic-liquid-based aqueous two-phase systems. *Sep. Purif. Technol.* **2014**, *128*, 58−66.
(62) Borges, G. A.; Silva, L. P.; Penido, J. A.; de Lemos, L. R.; Mageste, A. B.; Rodrigues, G. D. A method for dye extraction using an aqueous two-phase system: Effect of co-occurrence of contaminants in textile industry wastewater. *J. Environ. Manage.* **2016**, *183*, 196−203.
(63) Penido, J. A.; Mageste, A. B.; Martins, P. L.; Ferreira, G. M. D. Surfactant as selective modulator in the partitioning of dyes in aqueous two-phase systems: A strategy for separation. *J. Mol. Liq.* **2019**, *293*, 111501.
(64) Ivetic, D. Z.; Sciban, M. B.; Vasic, V. M.; Kukic, D. V.; Prodanovic, J. M.; Antov, M. G. Evaluation of possibility of textile dye removal from wastewater by aqueous two-phase extraction. *Desalination Water Treat.* **2013**, *51* (7−9), 1603−1608.
(65) Dilip, M.; Muthuraman, G.; Palanivelu, K. Removal of textile dyes from aqueous solution using PEG based aqueous biphasic system. *Toxicol. Environ. Chem.* **2005**, *87* (4), 499−507.
(66) Karma, V.; Gande, V. V.; Pushpavanam, S. Simultaneous extraction and enrichment of sunset yellow dye in an aqueous two-phase system. *Dyes Pigm.* **2023**, *212*, 111100.
(67) Raji, F.; Shayesteh, H.; Rahbar-Kelishami, A. Y.-Y. microfluidic polymer/salt aqueous two-phase system for optimization of dye extraction: Evaluation of channel geometry. *Sep. Sci. Technol.* **2022**, *57* (15), 2471−2481.
(68) de Alvarenga, J. M.; Fideles, R. A.; da Silva, M. V.; Murari, G. F.; Taylor, J. G.; de Lemos, L. R.; Dias Rodrigues, G.; Mageste, A. B. Partition study of textile dye Remazol Yellow Gold RNL in aqueous two-phase systems. *Fluid Phase Equilib.* **2015**, *391*, 1−8.
(69) Shiri, S.; Khezeli, T.; Lotfi, S.; Shiri, S. Aqueous Two-Phase Systems: A New Approach for the Determination of Brilliant Blue FCF in Water and Food Samples. *J. Chem.* **2013**, *2013*, 236196.

https://doi.org/10.1021/acs.jced.5c00346
J. Chem. Eng. Data 2025, 70, 3364−3377